J. Fluid Mech. (2015), *vol.* 774, *pp.* 324–341.

doi:10.1017/jfm.2015.241

The streamwise turbulence intensity in the intermediate layer of turbulent pipe flow

J. C. Vassilicos[1,2,4,†], J.-P. Laval[3,5], J.-M. Foucaut[2,5] and M. Stanislas[2,5]

[1]Department of Aeronautics, Imperial College London, London SW7 2AZ, UK

[2]ECLille, LML, F-59650 Villeneuve d'Ascq, France

[3]CNRS, UMR 8107, F-59650 Villeneuve d'Ascq, France

[4]USTL, LML, F-59650 Villeneuve d'Ascq, France

[5]Université Lille Nord de France, F-59000 Lille, France

(Received 1 August 2014; revised 19 March 2015; accepted 22 April 2015)

The spectral model of Perry *et al.* (*J. Fluid Mech.*, vol. 165, 1986, pp. 163–199) predicts that the integral length scale varies very slowly with distance to the wall in the intermediate layer. The only way for the integral length scale's variation to be more realistic while keeping with the Townsend–Perry attached eddy spectrum is to add a new wavenumber range to the model at wavenumbers smaller than that spectrum. This necessary addition can also account for the high-Reynolds-number outer peak of the turbulent kinetic energy in the intermediate layer. An analytic expression is obtained for this outer peak in agreement with extremely high-Reynolds-number data by Hultmark *et al.* (*Phys. Rev. Lett.*, vol. 108, 2012, 094501; *J. Fluid Mech.*, vol. 728, 2013, pp. 376–395). Townsend's (*The Structure of Turbulent Shear Flows*, 1976, Cambridge University Press) production–dissipation balance and the finding of Dallas *et al.* (*Phys. Rev.* E, vol. 80, 2009, 046306) that, in the intermediate layer, the eddy turnover time scales with skin friction velocity and distance to the wall implies that the logarithmic derivative of the mean flow has an outer peak at the same location as the turbulent kinetic energy. This is seen in the data of Hultmark *et al.* (*Phys. Rev. Lett.*, vol. 108, 2012, 094501; *J. Fluid Mech.*, vol. 728, 2013, pp. 376–395). The same approach also predicts that the logarithmic derivative of the mean flow has a logarithmic decay at distances to the wall larger than the position of the outer peak. This qualitative prediction is also supported by the aforementioned data.

Key words: pipe flow boundary layer, turbulent boundary layers, turbulent flows

1. Introduction

Considering turbulent pipe/channel and turbulent boundary layer flows, Townsend (1976) developed his well-known attached-eddy model to predict the profile with distance from the wall of the turbulent kinetic energy. This model is operative

† Email address for correspondence: j.c.vassilicos@imperial.ac.uk

in the intermediate range where the wall distance is much larger than the wall unit δ_ν and much smaller than, say, the pipe radius δ. In this intermediate range the turbulent kinetic energy scales with the square of the wall friction velocity u_τ and decreases logarithmically with distance to the wall. However, measurements in turbulent boundary layers dating from about 20 years ago (see Fernholz & Finley 1996) as well as more recent turbulent pipe flow measurements from the Princeton Superpipe (Morrison *et al.* 2004; Hultmark *et al.* 2012, 2013) show that an outer peak appears in the mean square fluctuating streamwise velocity at distances from the wall between about $100\delta_\nu$ and $800\delta_\nu$ when the turbulent Reynolds number $Re_\tau = \delta/\delta_\nu$ is larger than about 20 000. Such non-monotonic behaviour in regions where the mean velocity is monotonically increasing is hard to account for in current turbulence models and theory, and inconceivable within the current framework of Townsend's attached eddy model.

Starting with the spectral model of Perry, Henbest & Chong (1986) there have been numerous developments and extensions of the attached eddy model (see the review by Smits, McKeon & Marusic 2011 and references therein) but none has accounted for the outer peak in turbulent kinetic energy. Here we start from the observation (given in § 3) that the Perry *et al.* (1986) attached eddy model has a basic shortcoming to do with the integral length scale it predicts. There is only one way to repair this model without removing its attached eddy part, and this way naturally leads to an outer peak in turbulent kinetic energy.

In § 2 we provide some basic background on the type of turbulent pipe/channel flow considered in this paper and in § 3 we briefly describe the Townsend–Perry attached eddy model and its consequences on the integral scale. Section 4 is on the modification to the Townsend–Perry attached eddy model that we are forced to implement to remedy the integral scale problem. This section contains comparisons between the predictions of this modified attached eddy model and the Nano Scale Thermal Anemometry Probe (NSTAP) data obtained in the Princeton Superpipe by Hultmark *et al.* (2012, 2013). In § 5 we explain how intermittency in wall shear stress fluctuations could modify the attached-eddy k_1^{-1} spectrum and make it slightly steeper. In § 6 we predict that the logarithmic derivative of the mean flow must have an outer peak at the same distance from the wall where the turbulent kinetic energy has its outer peak and report that the data of Hultmark *et al.* (2012, 2013) show clear evidence of this. We end the paper with a list of main conclusions in § 7. The words 'turbulence intensity' appear in the title of this paper because it is concerned primarily with the mean square fluctuating streamwise velocity (§§ 3–5) but also with the streamwise mean flow (§ 6).

2. Turbulent pipe/channel flow

We consider a flow in a long enough smooth pipe/channel operating at high enough Reynolds number and steadily driven by a constant (in space and time) pressure gradient so that a turbulent region exists far enough from the inlet where turbulence statistics are independent of streamwise spatial coordinate x and of time t. The mean flow is $(\overline{u}, 0, 0)$ and the fluctuating velocity field is (u', v', w') where $\overline{u}$ and u' are along the streamwise axis and v' is parallel to the coordinate y normal to the wall. In the rest of the paper we refer to pipe flow only but our discussion applies to channel flow too.

The mean balance of forces along x, i.e. $-1/\rho(\mathrm{d}/\mathrm{d}x)\overline{P} = u_\tau^2/\delta$ where δ is the half-width of the channel or the radius of the pipe, allows determination of the skin friction velocity u_τ from measurements of the mean pressure gradient $-(\mathrm{d}/\mathrm{d}x)\overline{P}$ (ρ is the mass density of the fluid).

The wall unit is $\delta_\nu \equiv \nu/u_\tau$. It is well known that if the Reynolds number is large enough, then $\delta_\nu \ll \delta$, e.g. see Pope (2000). In such flows, one often uses the Reynolds number $Re_\tau \equiv \delta/\delta_\nu$ as reference. High Reynolds number then trivially implies wide separation of outer/inner length scales and an intermediate layer $\delta_\nu \ll y \ll \delta$ where y is the wall-normal spatial coordinate with $y = 0$ at the wall.

For a given channel/pipe (i.e. a given δ), a given fluid (i.e. a given kinematic viscosity ν), a given driving pressure drop (i.e. a given u_τ) and at a given distance y from the wall, a streamwise wavenumber k_1 could be comparable to $1/\delta$, $1/y$, $1/\eta$ or $1/\delta_\nu$ ($\eta \equiv (\nu^3/\epsilon)^{1/4}$ is the Kolmogorov microscale which is a function of y via its dependence on kinetic energy dissipation rate per unit mass ϵ).

The argument which shows that δ_ν is smaller than η is based on the log-law of the wall and on the direct balance between production and dissipation which one classically expects in the y-region where the Prandtl–von Kármán law of the wall holds, e.g. see Townsend (1976) and Pope (2000). At extremely high Re_τ, this balance may be written as $u_\tau^2(\mathrm{d}/\mathrm{d}y)\overline{u} \approx \epsilon$ where we have replaced the Reynolds stress by u_τ^2. It can be proved that the Reynolds shear stress is approximately equal to u_τ^2 in the range $\delta_\nu \ll y \ll \delta$. This follows from the turbulent pipe flow axial momentum balance and a very mild extra assumption, see § 3 of Dallas, Vassilicos & Hewitt (2009).

This equilibrium argument implies that $\epsilon \sim u_\tau^3/y$ (assuming that the log-law $(\mathrm{d}/\mathrm{d}y)\overline{u} \sim u_\tau/y$ holds) in $\delta_\nu \ll y \ll \delta$. It is now possible to compare $\eta = (\nu^3/\epsilon)^{1/4}$ and $\delta_\nu = \nu/u_\tau$ and it follows from $\delta_\nu \ll y$ that $1/\eta \ll 1/\delta_\nu$ in the range $\delta_\nu \ll y \ll \delta$. It is worth stressing that $1/\eta \ll 1/\delta_\nu$ and $\epsilon \sim u_\tau^3/y$ were obtained on the basis that the range $\delta_\nu \ll y \ll \delta$ is an equilibrium log-law range in a pipe flow. We revisit this assumption in § 6.

From the above arguments, where y is much larger than δ_ν but much smaller than δ, the axis of wavenumbers k_1 is marked by wavenumbers $1/\delta$, $1/y$, $1/\eta$ and $1/\delta_\nu$ in this increasing wavenumber order. This order of cross-over wavenumbers is important in the spectral interpretation given by Perry *et al.* (1986) of Townsend's attached eddy hypothesis.

3. The Townsend–Perry attached eddy model

Townsend (1976) assumed 'that the main, energy-containing motion is made up of contributions from "attached" eddies with similar velocity distributions' and developed a physical space argument based on the notion of a constant Reynolds shear stress which led to

$$\tfrac{1}{2}\overline{u'^2}(y)/u_\tau^2 \approx C_{s0} + C_{s1}\ln(\delta/y) \tag{3.1}$$

in the range $\delta_\nu \ll y \ll \delta$. The two constants C_{s0} and C_{s1} are independent of y and Re_τ.

Perry *et al.* (1986) developed a spectral attached eddy model and argued that where $\delta_\nu \ll y \ll \delta$, the streamwise energy spectrum $E_{11}(k_1, y)$ has three distinct ranges:

(i) $k_1 < 1/\delta$ where $E_{11}(k_1) \approx u_\tau^2 \delta g_o(k_1\delta)$ which must be $E_{11}(k_1) \approx C_\infty u_\tau^2 \delta$ with a constant C_∞ at small enough wavenumbers;

(ii) $1/\delta < k_1 < 1/y$ where $E_{11}(k_1) \approx C_0 u_\tau^2 k_1^{-1}$ (the 'attached eddy' range);

(iii) $1/y < k_1$ where $E_{11}(k_1)$ has the Kolmogorov form $E_{11}(k_1, y) \sim \epsilon^{2/3} k_1^{-5/3} g_K(k_1 y, k_1\eta)$, see Frisch (1995) and Pope (2000).

By integration of $E_{11}(k_1)$ they obtained for $\delta_\nu \ll y \ll \delta$

$$\tfrac{1}{2}\overline{u'^2}(y)/u_\tau^2 \approx C_\infty + C_0\ln(\delta/y) \tag{3.2}$$

where the constants C_∞ and C_0 are independent of y and Re_τ. Application of a strict matching condition for the energy spectra at $k_1 = 1/\delta$ gives $C_0 = C_\infty$ but this is of course not necessary. In fact, the constant C_∞ in (3.2) is not the same as the constant C_∞ in the spectral model if we allow for the wavenumber dependency of the outer function $g_o(k_1 y)$ and for the fact that this constant has a small contribution from the high-wavenumber Kolmogorov range (iii). The detail of this Kolmogorov contribution has been neglected in (3.2) as it only adds a term proportional to $1 - (y^+)^{-1/2}$ to the right-hand side ($y^+ \equiv y/\delta_\nu$) which is of little effect in the considered range.

A consequence of the Perry *et al.* (1986) model is that the integral scale L_{11} is proportional to δ and very weakly dependent on y in the intermediate layer $\delta_\nu \ll y \ll \delta$. This follows from $\pi E_{11}(k_1 = 0, y) = \overline{u'^2}(y) L_{11}(y)$ (see e.g. Tennekes & Lumley 1972) which leads to

$$L_{11}(y) \approx \frac{\pi C_\infty \delta}{C_\infty + C_0 \ln(\delta/y)} \tag{3.3}$$

where $\delta_\nu \ll y \ll \delta$. However, one expects that L_{11} may depend on y much more steeply. For example, the turbulent boundary layer measurements of Tomkins & Adrian (2003) suggest that $L_{11} \sim y$.

The only way for the Townsend–Perry attached eddy wavenumber range to be viable, i.e. the only way to have an integral scale which depends more substantially on y while keeping with the Townsend–Perry attached eddy wavenumber range (where, in particular, the constant C_0 is independent of y and Re_τ) is to modify the model of Perry *et al.* (1986) by inserting a fourth range to $E_{11}(k_1)$ between the very low-wavenumber range where $E_{11}(k_1) \approx C_\infty u_\tau^2 \delta$ and the 'attached eddy' range. We develop such a model in the following section.

4. A modified Townsend–Perry attached eddy model

We now consider a model of the energy spectrum $E_{11}(k_1, y)$ with the following four ranges (see figure 1)

(i) $k_1 < 1/\delta_\infty$ where $E_{11}(k_1) \approx C_\infty u_\tau^2 \delta$ with a constant C_∞ independent of wavenumber;
(ii) $1/\delta_\infty < k_1 < 1/\delta_*$ where $E_{11}(k_1) \approx C_1 u_\tau^2 \delta (k_1 \delta)^{-m}$ where $0 < m < 1$ and C_1 is also a constant independent of wavenumber;
(iii) $1/\delta_* < k_1 < 1/y$ where $E_{11}(k_1) \approx C_0 u_\tau^2 k_1^{-1}$ where C_0 is a constant independent of wavenumber, y and Re_τ (the 'attached eddy' range);
(iv) $1/y < k_1$ where $E_{11}(k_1)$ has the Kolmogorov form $E_{11}(k_1, y) \sim \epsilon^{2/3} k_1^{-5/3} g_K(k_1 y, k_1 \eta)$.

The new range which is dictated by the requirement of an integral scale significantly dependent on y is range (ii) and it lies, as is necessary for this requirement, between ranges (i) and the 'attached eddy' range (iii). This range therefore corresponds to rather large length scales which may naturally be expected to be the large and very large-scale motions first discovered by Tomkins & Adrian (2003) and confirmed for a range of Reynolds numbers by Hutchins & Marusic (2007) (see also Bailey & Smits 2010 in the present pipe flow context and the review of Smits *et al.* 2011). Indeed, such long regions of momentum deficit elongated in the streamwise direction should introduce long-range correlations in this direction. These long-range correlations will appear as a range of reduced rate of decline at the higher separation distances of the streamwise fluctuating velocity autocorrelation function which, when Fourier transformed, will give rise to a range such as range (ii) in the energy spectrum.

The bounds of the new range (ii) are determined by the two new length scales δ_∞ and δ_*. The only physics that we impose on them is the expectation that this range

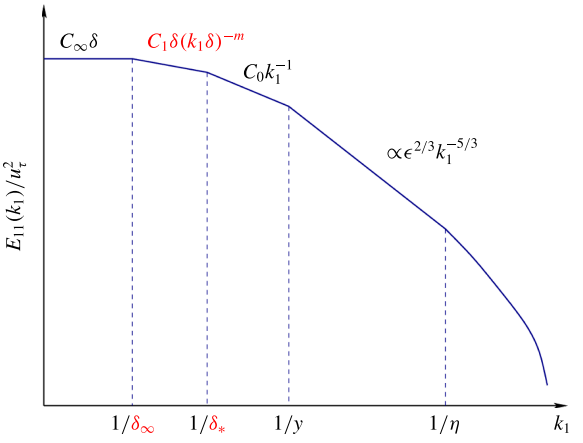

FIGURE 1. (Colour online) Schematic log–log plot of $E_{11}(k_1)/u_\tau^2$ versus k_1 according to the modified Townsend–Perry attached eddy model for the region $\delta_\nu \ll y \ll \delta$. Given an ansatz such as (4.1) with $p, q > 0$ and $p > q$ set by the physics described in the second and third paragraphs of § 4, the new range (ii) exists where $y < y_*$, in which case $\delta_* < \delta_\infty$, but does not exist where $y > y_*$ in which case the original Townsend–Perry model remains unaltered and $\delta_* = \delta_\infty = \delta$.

grows as y approaches the wall and distances itself from the centre of the pipe within $\delta_\nu \ll y \ll \delta$. The range $(1/\delta_*)/(1/\delta_\infty) = \delta_\infty/\delta_*$ can only depend on y, δ, ν and u_τ. Without loss of generality, it is therefore a function of y/δ and Re_τ or, equivalently, y^+ and Re_τ. At fixed Re_τ, δ_∞/δ_* must be a decreasing function of y/δ and also a decreasing function of y^+. At fixed y/δ, δ_∞/δ_* must be a decreasing function of Re_τ as this implies that y^+ increases. And at fixed y^+, δ_∞/δ_* must be an increasing function of Re_τ as this means that y/δ decreases.

An arbitrary but not impossible functional dependence is

$$\delta_\infty/\delta_* \approx A\,(y/\delta)^{-p} Re_\tau^{-q} \approx A(y^+)^{-p} Re_\tau{}^{p-q} \tag{4.1}$$

where A is a dimensionless constant. The qualitative physics which we described in the previous paragraph impose $p, q > 0$ and $p > q$. We adopt (4.1) indicatively in what follows as the aim of this work is to show the possibilities which open up with the adoption of the extra wavenumber range $1/\delta_\infty < k_1 < 1/\delta_*$ for the purpose of reconciling the Townsend–Perry attached eddy hypothesis with a more realistic integral length scale. We limit the values of the exponents p and q to $p, q > 0$ and $p > q$ without further constraints.

Matching of the energy spectral forms at $k_1 \approx 1/\delta_\infty$ gives $C_\infty = C_1(\delta/\delta_\infty)^{-m}$ and at $k_1 \approx 1/\delta_*$ gives $C_1 = C_0(\delta/\delta_*)^{m-1}$. It is not strictly necessary to impose these matching conditions as they unnecessarily restrict the cross-over forms of the energy spectra, but they do indicate that we need an expression for δ_*/δ if we are to proceed with or without them. Given that in all generality, δ_*/δ is a function of y/δ and Re_τ, we again assume a power-law form

$$\delta_*/\delta = B\,(y/\delta)^\alpha Re_\tau^\beta \tag{4.2}$$

where, like A, B is a dimensionless constant.

There are also two requirements for the viability of our spectra: $y \ll \delta_*$ and $\delta_* < \delta_\infty$. The former is met provided that $\beta \geqslant \alpha - 1$ for $y \gg \delta_\nu$. The latter is met if $y < y_* \equiv \delta A^{1/p} Re_\tau^{-q/p}$.

We therefore adopt the new range (ii) for $y < y_*$ but keep the Perry *et al.* (1986) model unaltered for $y > y_*$. Their model can indeed remain unaltered if $\delta_\infty = \delta_* = \delta$ at $y \geqslant y_* = \delta A^{1/p} Re_\tau^{-q/p}$. The continuous passage from (4.1) and (4.2) to $\delta_\infty = \delta_* = \delta$ requires $\beta = \alpha q/p$ and $BA^{\alpha/p} = 1$.

By integration of $E_{11}(k_1)$ we obtain for $\delta_\nu \ll y \leqslant y_*$

$$\tfrac{1}{2}\overline{u'^2}(y)/u_\tau^2 \approx C_{s0} - C_{s1} \ln(\delta/y) - C_{s2}(y/\delta)^{p(1-m)} Re_\tau^{q(1-m)} \tag{4.3}$$

where $C_{s0} = (C_0/(1-m)) + C_0 \ln B + C_0 \alpha (q/p) \ln Re_\tau$, $C_{s1} = C_0(\alpha - 1)$ and $C_{s2} = (mC_0 A^{m-1})/(1-m)$. (Note that C_{s0} is a weak function of Re_τ whereas C_{s1} and C_{s2} are independent of Re_τ.) These new constants have been calculated by taking into account the perhaps over-constraining matching conditions $C_\infty = C_1(\delta/\delta_\infty)^{-m}$ and $C_1 = C_0(\delta/\delta_*)^{m-1}$.

The integral length scale is now

$$L_{11}/\delta = \pi C_0 A^m B (y/\delta)^{\alpha - pm} Re_\tau^{\beta - qm} / (\overline{u'^2}(y)/u_\tau^2) \tag{4.4}$$

clearly more strongly dependent on y than in (3.3).

Equation (4.3) can be compared with the Townsend–Perry form which remains valid here for $y_* \leqslant y \ll \delta$ and which is (taking $C_\infty = C_0$)

$$\tfrac{1}{2}\overline{u'^2}(y)/u_\tau^2 \approx C_0 + C_0 \ln(\delta/y). \tag{4.5}$$

The two profiles (4.3) and (4.5) match at $y = y_* \equiv \delta A^{1/p} Re_\tau^{-q/p}$ and so do also the integral length-scale forms (4.4) and (3.3) if $C_\infty = C_0$. Our approach does not modify the Townsend–Perry form of L_{11} at large distances from the wall, i.e. at $y > y_*$, but it does return a significant dependence of L_{11} on y which, however, is arbitrarily set by (4.1) and (4.2). Even so, the possibility is now open for a stronger dependence of L_{11} on y. This possibility has been opened by the adoption of an extra wavenumber range $1/\delta_\infty < k_1 < 1/\delta_*$ which, in turn, returns a form of the $\overline{u'^2}(y)$ profile which allows for a maximum value (a peak) inside the intermediate region $\delta_\nu \ll y \ll \delta$. No such peak is allowed by the Townsend–Perry forms (3.1) and (3.2) although such a peak has been observed in measurements of both turbulent boundary layers and turbulent pipe flows over the past 20 years or so, see Fernholz & Finley (1996), Morrison *et al.* (2004) and Hultmark *et al.* (2012, 2013). It has been suggested that this peak is associated with the large and very large motions (see Smits *et al.* 2011 and references therein) which is consistent with the view that the wavenumber range $1/\delta_\infty < k_1 < 1/\delta_*$ results from these very elongated streamwise structures.

Straightforward analysis of (4.3) shows that a maximum streamwise turbulence intensity does exist in the range $\delta_\nu \ll y \ll \delta$ if $0 < \alpha - 1 < pm$ (i.e. if $C_{s1} > 0$ and $\alpha < pm + 1$) and that the position y_{peak} of this maximum is

$$y_{peak}/\delta \sim Re_\tau^{-q/p} \tag{4.6}$$

which decreases with increasing Re_τ and, equivalently,

$$y_{peak}/\delta_\nu \sim Re_\tau^{1-q/p} \tag{4.7}$$

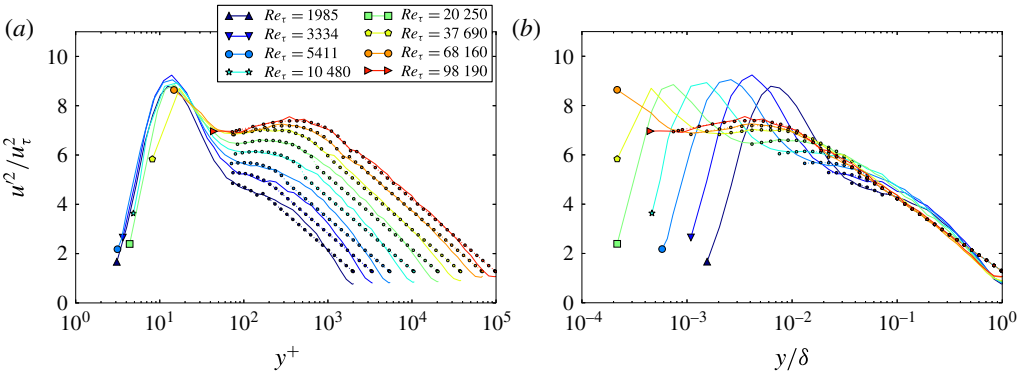

FIGURE 2. (Colour online) Plots of $\overline{u'^2}(y)/u_\tau^2$ versus y^+ (*a*) and y/δ (*b*) obtained from the NSTAP Superpipe data of Hultmark *et al.* (2012, 2013) for different values of Re_τ. The circles are calculated from (4.5) and (4.9) with $C_0 = 1.28$, $y_* = \delta Re_\tau^{-d_2/d_1}$ for all Reynolds numbers and the values of d_1 and d_2 and the constants in (4.9) given in figure 3.

which increases with increasing Re_τ as $q < p$. It also follows from (4.3) that

$$\frac{\mathrm{d}}{\mathrm{d}\ln Re_\tau}\left(\frac{1}{2}\overline{u'^2}(y_{peak})/u_\tau^2\right) \approx C_0(\alpha p/q - \alpha q/p + q/p) > 0. \tag{4.8}$$

The maximum value of $\overline{u'^2}(y)/u_\tau^2$ at $y = y_{peak}$ therefore grows logarithmically with increasing Re_τ.

We now compare our functional dependence of $(\overline{u'^2}(y)/2)/u_\tau^2$ on y and Re_τ with smooth wall turbulent pipe flow data obtained recently with a new NSTAP by Hultmark *et al.* (2012, 2013). Below we refer to this data as NSTAP Superpipe data.

We start by fitting the data with (4.5) in the range $y_* < y \ll \delta$ and

$$\tfrac{1}{2}\overline{u'^2}(y)/u_\tau^2 \approx C_{s0} - C_{s1}\ln(\delta/y) - C_{s2}(y/\delta)^{d_1}Re_\tau^{d_2} \tag{4.9}$$

instead of (4.3) in the range $\delta_\nu \ll y < y_*$ where $y_* = \delta Re_\tau^{-d_2/d_1}$. This is a model where we ignore the various matching conditions which led to (4.3) with the specific relations between C_{s0}, C_{s1} and C_{s2} and the parameters C_0, m, p, q, A, α and Re_τ. It is also a model where we just set $A = 1$, $d_1 = p(1-m)$ and $d_2 = q(1-m)$ so that $y_* = \delta Re_\tau^{-d_2/d_1}$. In figure 2 we show the result of this fit against the NSTAP Superpipe data and in figure 3 we show the fitting values of C_{s0}, C_{s1}, C_{s2} and d_1 and d_2 and their dependence on Re_τ in a lin-log plot.

First note in figure 2 the clear presence when Re_τ is larger than about 20 000 of a logarithmic region at the higher y-values in agreement with the Townsend–Perry equation (4.5) which fits it quite well (the fit is much better if we allow C_∞ to be different from C_0 as in (3.2)). This was of course already noted by Hultmark *et al.* (2012, 2013). Second note the gradual development as Re_τ increases of a peak of turbulence intensity inside the intermediate region $\delta_\nu \ll y \ll \delta$. This outer peak is distinct from the well-known near-wall peak at $y^+ \approx 15$ and starts appearing clearly at Re_τ larger than about 20 000. Of course this was also noted in Hultmark *et al.* (2012, 2013) who pointed out that the position y_{peak} of the outer peak depends on Reynolds number as $y_{peak}/\delta_\nu \approx 0.23Re_\tau^{0.67}$. In terms of our model this means $d_2/d_1 = q/p \approx 1/3$.

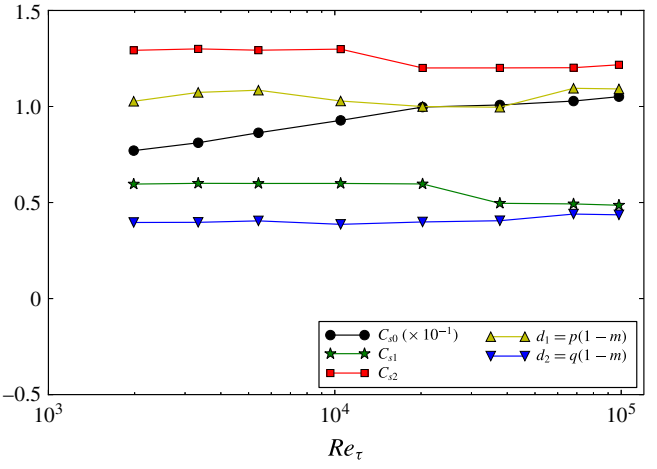

FIGURE 3. (Colour online) Model parameters C_{s0}, C_{s1}, C_{s2}, d_1 and d_2 appearing in (4.9). Plotted as functions of Re_τ.

As predicted by the physics instilled in our model (see the paragraph containing (4.1) and the paragraph preceding it) y_{peak}/δ decreases and y_{peak}/δ_ν increases with increasing Re_τ (see figure 2). As also predicted by the physics of our model, the value of $\overline{u'^2}/u_\tau^2$ at the outer peak slowly increases with increasing Re_τ and the fits in figure 2 which we discuss in the following paragraph indicate that this increase is indeed only logarithmic as in (4.8).

The point $y = y_*$ is clearly seen in figure 2 because we did not adopt matching conditions to ensure a continuous passage from (4.9) to (4.5). Nevertheless the new (4.9) returns a satisfactory fit of the outer peak, including its shape, intensity and location. In figure 3 we plot the Reynolds number dependence of the constants C_{s0}, C_{s1} and C_{s2}, d_1 and d_2 involved in these fits. Note how the parameters C_{s1}, C_{s2}, d_1 and d_2 do not deviate much from a constant value except for C_{s0} which grows slowly with Re_τ, in fact approximately linearly with $\ln Re_\tau$ as in prediction (4.3).

In figure 4 we fit the NSTAP Superpipe data with (4.5) in the range $y_* < y \ll \delta$ and (4.3) in the range $\delta_\nu \ll y < y_*$ where $y_* = \delta A^{1/p} Re_\tau^{-q/p}$ and with C_{s0}, C_{s1} and C_{s2} given by

$$C_{s0} = \frac{C_0}{1-m} + C_0 \ln B + C_0 \alpha \frac{q}{p} \ln Re_\tau, \tag{4.10}$$

$$C_{s1} = C_0(\alpha - 1), \tag{4.11}$$

$$C_{s2} = \frac{m C_0 A^{m-1}}{1-m} \tag{4.12}$$

where $B = A^{\alpha/p}$ as obtained above in the text between (4.2) and (4.3). The fits in figure 4 are obtained for $A = 0.2$, $C_0 = 1.28$, $m = 0.37$, $q = 0.79$, $p = 2.38$ and $\alpha = 1.21$. It works rather well, although not perfectly, for Re_τ larger than about 30 000. Note that we did not optimise the choice of our fitting parameters to obtain the best possible fit. As things stand, (4.9) fits better the outer peak than (4.3) with (4.10)–(4.12) and $B = A^{\alpha/p}$. However, as of course expected, the latter over-matched model returns a continuous transition to (4.5) at $y = y_*$. Note that $y_{peak} \approx 0.45\, y_*$ (from $y_{peak}/\delta_\nu \approx 0.23\, Re_\tau^{0.67}$ and $y_* = \delta A^{1/p} Re_\tau^{-q/p}$).

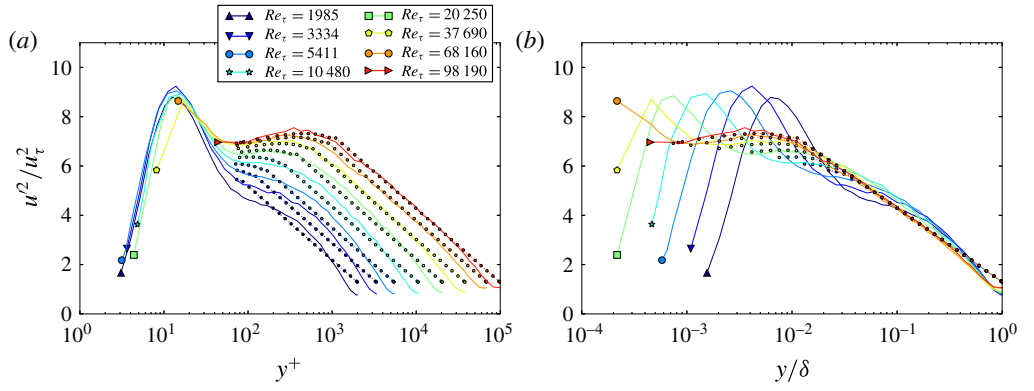

FIGURE 4. (Colour online) Plots of $\overline{u'^2}(y)/u_\tau^2$ versus y^+ (*a*) and y/δ (*b*) obtained from the NSTAP Superpipe data of Hultmark *et al.* (2012, 2013) for different values of Re_τ. The circles are calculated for all Reynolds numbers from (4.5) and (4.3) with $y_* = \delta A^{1/p} Re_\tau^{-q/p}$ and $A = 0.2$, $C_0 = 1.28$, $m = 0.37$, $q = 0.79$, $p = 2.38$ and $\alpha = 1.21$.

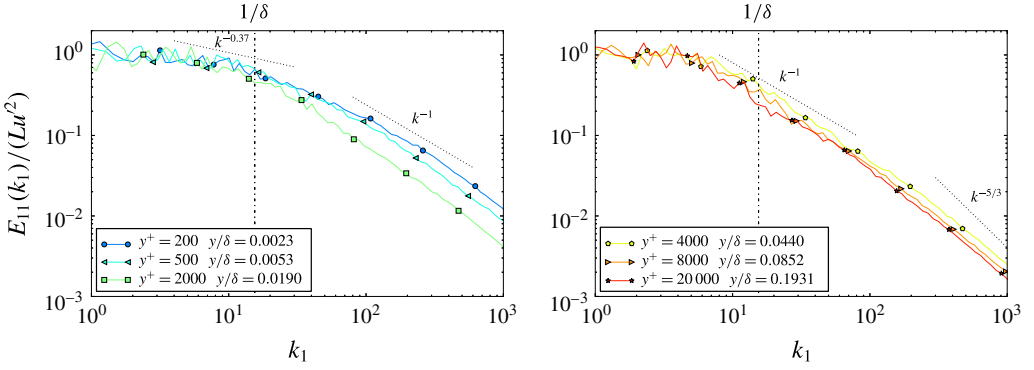

FIGURE 5. (Colour online) NSTAP Superpipe energy spectra $E_{11}(k_1, y)$ at various distances from the wall for $Re_\tau = 98\,190$. At this Reynolds number, $y_*/\delta_\nu \approx 2130$. The spectra are normalised by $\overline{u'^2}(y)L_{11}(y)$ where $L_{11}(y)$ are the integral scales obtained from these spectra.

Indicatively and only for illustrative purposes, we mention that the fits in figure 4 correspond, approximately (we have rounded off the exponents to make them look like fractions without any intention to suggest a deeper level of theory), to $\delta_\infty/\delta_* \approx 0.2(y/\delta)^{-7/3} Re_\tau^{-4/5}$ and $\delta_* \approx 2.26\delta(y/\delta)^{6/5} Re_\tau^{2/5}$ given that $\beta = \alpha q/p$. The model leading to these particular fits also effectively assumes that the longitudinal spectra in the region $\delta_\nu \ll y < y_* \approx 0.5\delta Re_\tau^{-1/3}$ have a range of wavenumbers $1/\delta_\infty < k_1 < 1/\delta_*$ which are lower than the usual attached eddy ones and where $E_{11}(k_1) \approx (2/3)u_\tau^2 y Re_\tau^{1/3}(k_1\delta)^{-1/3} = (2/3)u_\tau^2 y(k_1\delta_\nu)^{-1/3}$. Note the presence of both y and δ_ν in these particularly low-wavenumber spectra. Note also that $\delta_* < 0.2\delta$ and $\delta_\infty > 5\delta/100$ given that $y < y_* \approx 0.5\delta Re_\tau^{-1/3}$. Finally, $y_* > 15\delta_\nu$ as long as $Re_\tau > 165$.

In the region $y_* \approx 0.5\delta Re_\tau^{-1/3} < y \ll \delta$ no such spectral range exists; only the attached eddy form $E_{11} \approx 1.28 u_\tau^2 k_1^{-1}$ is present in the usual range $1/\delta < k_1 < 1/y$. The constant $C_0 = 1.28$ is the one used to fit the data in both figures 4 and 2.

Figure 5 shows spectra plotted indicatively as wavenumber spectra at many distances from the wall for a value of Re_τ equal to 98 190 and $y_*/\delta_\nu \approx 2130$. These

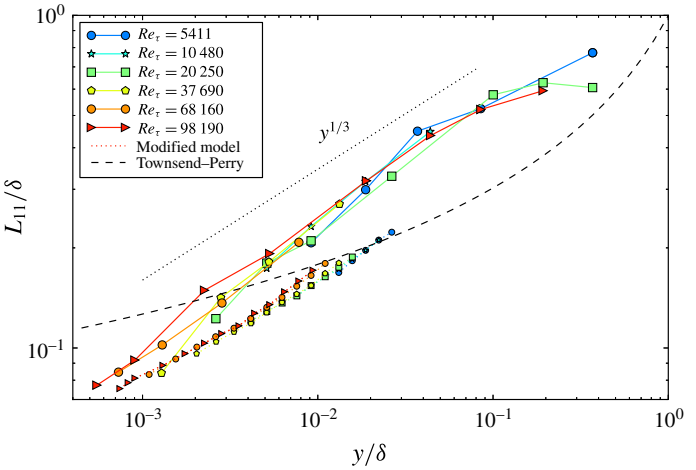

FIGURE 6. (Colour online) Normalised integral scales L_{11}/δ obtained from NSTAP Superpipe energy spectra plotted versus y/δ for various Reynolds numbers. Also plotted are the Townsend–Perry and our modified model's prediction for L_{11}/δ.

spectra are really frequency spectra as we cannot expect the Taylor hypothesis to be accurate enough at the lower wavenumbers and at the closer positions to the wall. With this serious caveat firmly in mind it is nevertheless intriguing to see in figure 5 that very high-Reynolds-number spectra do indeed have an extra low-frequency range at $y < y_*$ where the spectrum is much shallower than k_1^{-1} yet not constant; and that this range is absent at higher positions from the wall where $y > y_*$. At distances y from the wall larger than y_* one sees a spectral wavenumber dependence which is close to k_1^{-1} (perhaps a little steeper) between a very low-wavenumber constant spectrum and a very high-wavenumber spectrum which is much steeper than k_1^{-1}, perhaps close to $k_1^{-5/3}$. Even the deviation from the k_1^{-1} spectrum which makes it look a little steeper could be a frequency domain signature which does not quite correspond to k_1^{-1} because of Taylor hypothesis failure, see del Alamo & Jimenez (2009) but also Rosenberg *et al.* (2013).

Our initial motivation for modifying the Perry *et al.* (1986) model and adding an extra spectral range to it was the y-dependence of the integral scale. The values of the exponents α, q, p and m used in the fits of figure 4 combined with the constraint $\beta = \alpha q/p$ are such that $L_{11}/\delta \sim (y/\delta)^{1/3} Re_\tau^{0.1}$ if we neglect the logarithmic dependence of $\overline{u'^2}(y)/u_\tau^2$ in (4.4). In figure 6 we plot L_{11}/δ versus y/δ as obtained from the lowest frequencies of the NSTAP Superpipe spectra (see for example figure 5) for different Reynolds numbers. Again, the integral scales plotted in figure 6 should be taken with much caution and only very indicatively as they are really integral time scales and the Taylor hypothesis cannot be invoked at these low frequencies. In that same figure we nevertheless plot the Townsend–Perry formula (3.3) where $C_\infty = C_0$ as per the fitting constants for figure 4 (i.e. $L_{11} \approx \pi\delta/(1 + \ln(\delta/y))$) and formula (4.4). In (4.4) we used the fitting constants that we also used for the fits in figure 4. Note that (4.4) is defined for y in the range $\delta_\nu \ll y < y_* = 0.5\delta Re_\tau^{-1/3}$ and that, even in the modified model, L_{11} is given by (3.3) in the range $y_* \ll y < \delta$. The points in figure 6 where the modified model curves meet the Townsend–Perry curve are at $y = y_*$ for the different Re_τ. It is clear that the modified model succeeds in steepening the y-dependence of

L_{11} in the range $\delta_\nu \ll y < y_*$ and that it keeps the original y-dependence of L_{11} in the range $y_* \ll y < \delta$. It is also clear, though, that formulae (4.4) and (3.3) do not match the NSTAP Superpipe integral scales well with the fitting constants used for figure 4. We repeat that the integral scales obtained from the NSTAP Superpipe data are really integral time scales and it is not clear that they should be proportional to L_{11}. If such a proportionality could be established, however, then the data would indicate that $L_{11}/\delta \sim (y/\delta)^{1/3}$ for all Reynolds numbers in some agreement with our modified model's $L_{11}/\delta \sim (y/\delta)^{1/3} Re_\tau^{0.1}$, but the constants of proportionality are different.

Finally, we draw attention to the fact that the integral scale L_{11} is not proportional to y in the range $\delta_\nu \ll y \ll \delta$ as one might have expected (see Tomkins & Adrian 2003 who found several spanwise length scales, including L_{11}, to be proportional to y in a turbulent boundary layer).

5. Intermittent attached eddies

We now address the possibility brought up by experimental results such as figure 5 that, in the appropriate Townsend–Perry attached eddy range of wavenumbers, the energy spectra may not scale as k_1^{-1} but as a slightly steeper power of k_1. As pointed out by del Alamo & Jimenez (2009), observed deviations from k_1^{-1} could result from a failure of the Taylor hypothesis, a point which we do not dispute. However, we show in this section that slightly steeper powers of k_1 can also arise because of intermittent fluctuations of the wall shear stress, as observed for example by Alfredsson *et al.* (1988) and Örlü & Schlatter (2011).

One way to argue, in the region $\delta_\nu \ll y \ll \delta$, that $E_{11}(k_1, y) \sim u_\tau^2 k_1^{-1}$ in the wavenumber range $1/\delta \ll y \ll 1/y$ is by hypothesising that the attached eddies dominate the spectrum in that range independently of y and that these eddies are themselves dominated by the wall shear stress, i.e. the skin friction, at the wall. Hence, $E_{11}(k_1, y)$ can only depend on u_τ^2 and k_1 in the region $\delta_\nu \ll y \ll \delta$, which implies that $E_{11}(k_1, y) \sim u_\tau^2 k_1^{-1}$.

We now show how this argument can be modified to take into account the intermittency in the wall shear stress. To do this we adopt the way that Kolmogorov (1962) took into account the inertial-range intermittency of kinetic energy dissipation in homogeneous turbulence and adapt it to the intermittency of wall shear stress in wall turbulence. We therefore define the scale-dependent filter averages

$$u_*^2(x, r, t) = \frac{1}{2r} \int_{x-r}^{x+r} \nu \left.\frac{\mathrm{d}u}{\mathrm{d}y}\right|_{wall} (x, t)\, \mathrm{d}x. \tag{5.1}$$

Following Kolmogorov's (1962) approach we assume that the statistics of $u_*^2(x, r, t)$ are lognormal at scales r large enough for $u_*^2(x, r, t)$ to be reasonably presumed positive. It may be reasonable to assume scales r much larger than y to be such scales if $\delta_\nu \ll y \ll \delta$. For such scales we therefore define $\xi_r \equiv \ln(u_*^2/u_\tau^2)$ and assume ξ_r to be a Gaussian-distributed random variable, i.e. its probability distribution function (PDF) is

$$P(\xi_r) = \frac{1}{\sqrt{2\pi}\sigma_r} \mathrm{e}^{-(\xi_r - m_r)^2/2\sigma_r^2}. \tag{5.2}$$

The constraint $\langle u_*^2(x, r, t)\rangle = u_\tau^2$ implies $m_r = -\sigma_r^2/2$ (the angular brackets signify an average over time or over x or both). The exact form of this PDF does not really matter as we are only concerned with low-order moments.

We now hypothesise that, in the appropriate Townsend–Perry attached eddy range of wavenumbers, the average of $(u'(x+r,y)-u'(x,y))^2$ conditioned on a given value of $u_*^2(x,r,t)$ depends only on that value and r (u' is the streamwise fluctuating turbulence velocity component). By dimensional analysis the dependence on r drops out, and as the structure function $\langle(u'(x+r,y)-u'(x,y))^2\rangle$ is the average over all of these conditional averages, we are left with $\langle(u'(x+r,y)-u'(x,y))^2\rangle \sim \langle u_*^2(x,r,t)\rangle$. Using (5.2) to calculate this average, we obtain

$$\langle(u'(x+r,y)-u'(x,y))^2\rangle \sim u_\tau^2 \int \mathrm{d}\xi \, \frac{\mathrm{e}^{\xi}}{\sqrt{2\pi}\sigma_r} \mathrm{e}^{-(\xi-m_r)^2/2\sigma_r^2} \sim u_\tau^2 \mathrm{e}^{-\sigma_r^2/9}. \tag{5.3}$$

A logarithmic dependence of σ_r^2 on r, for example $\sigma_r^2 = \text{const.} + 9\mu \ln(\delta/r)$ where $\mu > 0$, returns $\langle(u'(x+r,y)-u'(x,y))^2\rangle \sim u_\tau^2 (r/\delta)^{\mu}$, i.e.

$$E_{11}(k_1,y) \sim u_\tau^2 \delta (k_1\delta)^{-1-\mu}. \tag{5.4}$$

This demonstrates that the attached eddy hypothesis suitably modified to take into account the intermittent fluctuations of the wall shear stress can lead to spectra that are slightly steeper than k_1^{-1}. The statistics of the intermittently fluctuating wall shear stress can therefore have some bearing on energy spectra and, in turn, on vertical profiles of the turbulent kinetic energy. One can readily see that replacement of $E_{11}(k_1,y) \approx C_0 u_\tau^2 k_1^{-1}$ by $E_{11}(k_1,y) \approx C_0 u_\tau^2 \delta (k_1\delta)^{-1-\mu}$ in range (ii) of the Perry *et al.* (1986) model (§ 3) and in range (iii) of our modified model (§ 4) would lead to profiles such as (4.5) and (4.9) where the $\ln(\delta/y)$ terms would be replaced by weak power laws of y/δ. However, for very small exponents μ this difference would be very hard to detect experimentally.

6. The mean flow profile

As already noted by Townsend (1976), the attached eddy hypothesis is incompatible with the assumption that $\mathrm{d}\overline{u}/\mathrm{d}y$ is independent of δ. This assumption is required to argue that $\mathrm{d}\overline{u}/\mathrm{d}y$ depends only on y and u_τ in the range $\delta_\nu \ll y \ll \delta$. As $Re_\tau \to \infty$ an intermediate layer $\delta_\nu \ll y \ll \delta$ does emerge, however, where something may nevertheless be independent of ν and δ. Dallas *et al.* (2009) presented evidence from direct numerical simulations (DNS) of turbulent channel flow which shows that the eddy turnover time $\tau \equiv E/\epsilon$ (where E is the total turbulent kinetic energy) is proportional to y/u_τ in the range $\delta_\nu \ll y \ll \delta$ for a variety of moderate values of Re_τ.

Here we make the reasonable extrapolation that the observation of Dallas *et al.* (2009) is not limited to moderate Reynolds numbers and that τ is independent of ν and δ at all large enough Reynolds numbers. Hence, $\tau \sim y/u_\tau$ in the range $\delta_\nu \ll y \ll \delta$ for turbulent pipe flows.

Following Townsend (1976) we also assume local balance between production and dissipation, i.e. $-\langle u'v'\rangle(\mathrm{d}\overline{u}/\mathrm{d}y) \approx \epsilon = E/\tau$, but only in a region $y_{P\epsilon} < y \ll \delta$ where $\delta_\nu \ll y_{P\epsilon}$. Making use of the well-known axial momentum balance in turbulent pipe flow, see Pope (2000),

$$\nu \frac{\mathrm{d}}{\mathrm{d}y}\overline{u} - \langle u'v'\rangle = u_\tau^2(1-y/\delta), \tag{6.1}$$

and introducing the constant C_s in $\tau \approx C_s(y/u_\tau)$, we are led to

$$\left(1 - y/\delta - \frac{\mathrm{d}\overline{u}_+}{\mathrm{d}y^+}\right) \frac{\mathrm{d}\overline{u}_+}{\mathrm{d}\ln y^+} \approx C_s E/u_\tau^2 = C_s E^+ \tag{6.2}$$

in the region $y_{P\epsilon} < y \ll \delta$.

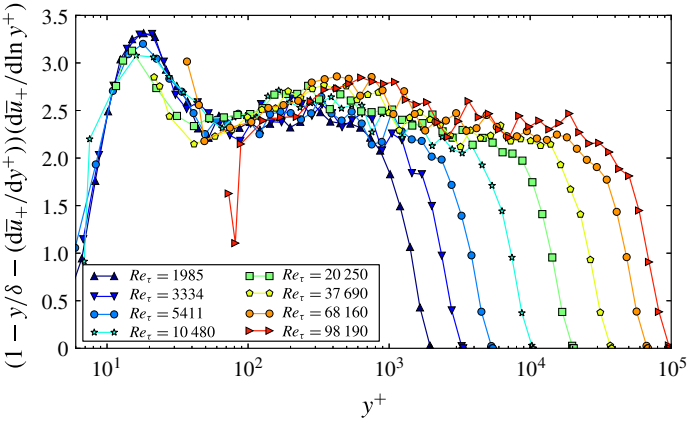

FIGURE 7. (Colour online) Linear-logarithmic plot of $(1-y/\delta-(\mathrm{d}\overline{u}_+/\mathrm{d}y^+))(\mathrm{d}\overline{u}_+/\mathrm{d}\ln y^+)$ versus y^+ for different values of Re_τ obtained from the NSTAP Superpipe mean flow data of Hultmark *et al.* (2012, 2013).

We know from the Townsend–Perry attached eddy model and also from this paper's modified model that $E^+ \approx M_0 + M_1 \ln(\delta/y)$ in the range $y_* < y \ll \delta$ where M_0 and M_1 are constants different from C_∞ and C_0 in (3.2) because one needs to also take into account $(\overline{w'^2}(y)/2)/u_\tau^2$ and $(\overline{v'^2}(y)/2)/u_\tau^2$. Hence, the first prediction of our approach based on $\tau \approx C_s(y/u_\tau)$ and $-\langle u'v'\rangle(\mathrm{d}\overline{u}/\mathrm{d}y) \approx \epsilon$ is that the left-hand side of (6.2) is approximately equal to $C_sM_0 + C_sM_1 \ln(\delta/y)$ in $y_* < y \ll \delta$.

If E^+ has an outer peak at the same $y = y_{peak}$ location as $(\overline{u'^2}(y)/2)/u_\tau^2$ and if $y_{P\epsilon} < y_{peak}$ then the second prediction of our approach is that the left-hand side of (6.2) has an outer peak at $y = y_{peak}$.

Figure 7 is a plot of the left-hand side of (6.2) based on the NSTAP Superpipe data of Hultmark *et al.* (2012, 2013). This plot suggests that there is indeed an outer peak in the functional dependence on y of the left-hand side of (6.2). It is also not inconsistent with the prediction that the left-hand side of (6.2) is a logarithmically decreasing function of y for much of the region where y is greater than the location of this outer peak. Figure 8 shows this left-hand side for the higher Re_τ NSTAP Superpipe data (Re_τ between 20 000 and 100 000). There is no evidence that the left-hand side of (6.2) decreases logarithmically with y for the lower Reynolds numbers in figure 7, in agreement with (6.2) and figures 2 and 4 which show that there is no such logarithmic decrease in $(\overline{u'^2}(y)/2)/u_\tau^2$ either at $Re_\tau < 10\,000$. However, such a y-dependence is not inconsistent with much of the y-dependence for the $Re_\tau > 20\,000$ data at the right of the outer peak in figure 8.

In figure 9 we replot the high-Re_τ data of figure 8 but as functions of y/δ in one plot and of y/y_{peak} in the other. These plots demonstrate that the position of the outer peak in the left-hand side of (6.2) is the same as the position of the outer peak in $(\overline{u'^2}(y)/2)/u_\tau^2$. And they also demonstrate that the left-hand side of (6.2), if indeed logarithmically decreasing, is approximately equal to $C_sM_0 + C_sM_1 \ln(\delta/y)$ in $y_* < y \ll \delta$ (though the data in our disposal do not permit us to check that the constants C_sM_0 and C_sM_1 are indeed the products of C_s with M_0 and M_1 respectively).

In figure 10 we use the NSTAP Superpipe data to plot $(1-y/\delta-(\mathrm{d}\overline{u}_+/\mathrm{d}y^+))$ as a function of y/δ in one case and y^+ in the other. As these are pipe data, the plots in figure 10 are effectively plots of the normalised Reynolds stress $-\langle u'v'\rangle/u_\tau^2$. It is

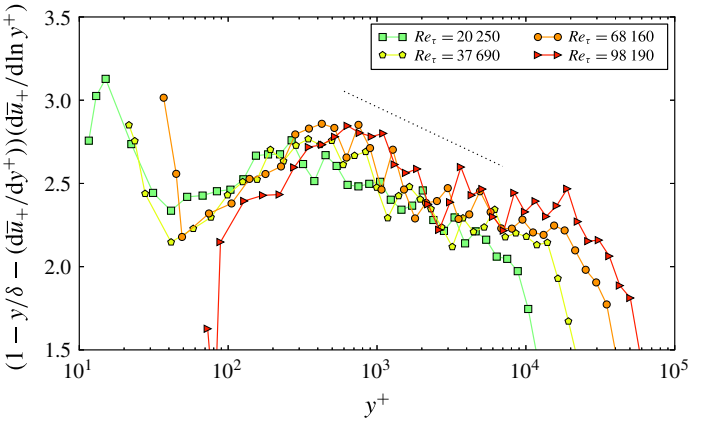

FIGURE 8. (Colour online) Blow up of figure 7 for the four highest Reynolds numbers with a superposed dotted line suggesting logarithmic dependence of $(1 - y/\delta - (\mathrm{d}\overline{u}_+/\mathrm{d}y^+))(\mathrm{d}\overline{u}_+/\mathrm{d}\ln y^+)$ on y at the right of the peak.

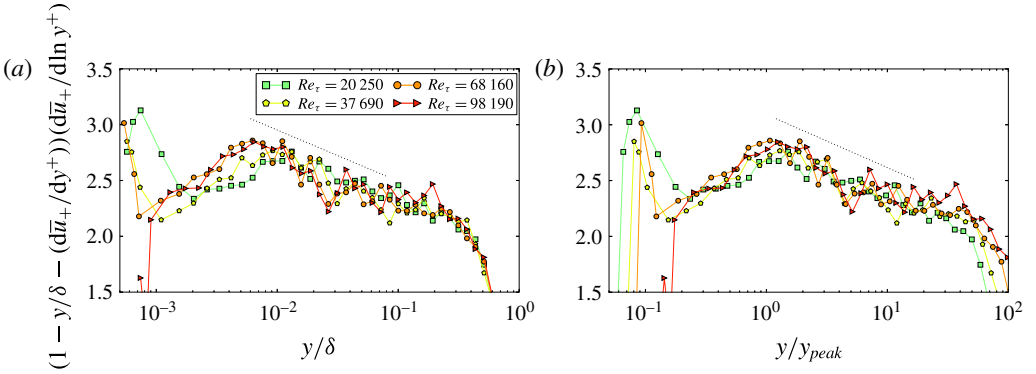

FIGURE 9. (Colour online) Blow ups of figure 7 for the four highest Reynolds numbers plotted versus y/δ (*a*) and versus y/y_{peak} (*b*) where $y_{peak} = 0.23\delta_\nu Re_\tau^{0.67}$ is the fit by Hultmark *et al.* (2012) of the location of the outer peak in the streamwise turbulent energy plotted in figures 2 and 4. The superposed dotted line suggests a logarithmic dependence of $(1 - y/\delta - (\mathrm{d}\overline{u}_+/\mathrm{d}y^+))(\mathrm{d}\overline{u}_+/\mathrm{d}\ln y^+)$ on y/δ at the right of the peak.

clear that $-\langle u'v'\rangle \approx u_\tau^2$ only if $Re_\tau > 40\,000$ and for distances from the wall such that $100 < y^+$ and $y/\delta < 0.01$. (See also Zhao & Smits 2007 who showed that the viscous contribution to the total stress is less that 1 % at $y^+ > 250$.) It of course remains perfectly true that $-\langle u'v'\rangle/u_\tau^2$ is a linear function of y/δ at a distance of a few hundred wall units from the walls but it is also true that this linear dependence is small compared to 1 (the leading term) for y/δ smaller than $O(10^{-2})$. The resulting intermediate range of wall distances y where $-\langle u'v'\rangle \approx u_\tau^2$ is a good approximation requires Re_τ to be larger than $O(10^4)$ to exist. At values of y larger than $\delta/10$ the normalised Reynolds stress decreases abruptly towards 0 which explains why the left-hand side of (6.2) does the same in figures 7–9 at these values of y.

Figure 10 makes it clear that (6.2) simplifies to

$$\frac{\mathrm{d}\overline{u}_+}{\mathrm{d}\ln y^+} \approx C_s E^+ \tag{6.3}$$

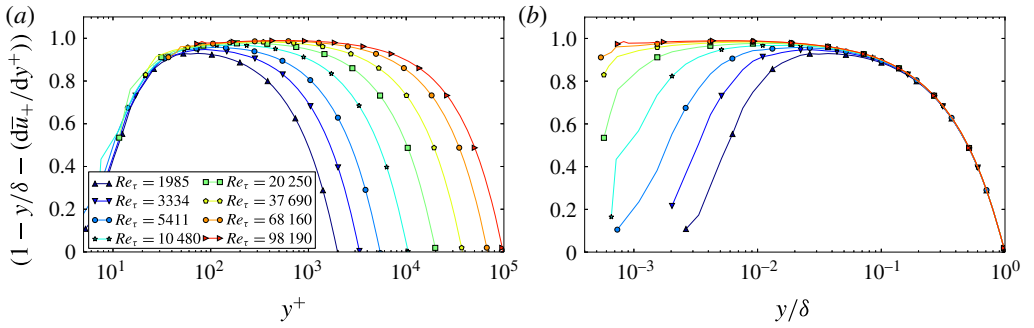

FIGURE 10. (Colour online) Normalised Reynolds stress $-\langle u'v'\rangle/u_\tau^2$ calculated from the NSTAP Superpipe mean flow data of Hultmark *et al.* (2012, 2013) as $(1 - y/\delta - (\mathrm{d}\overline{u}_+/\mathrm{d}y^+))$ (for turbulent pipe flow) versus y^+ (*a*) and versus y/δ (*b*). Here Re_τ ranges from about 2000 to about 100 000.

in turbulent pipe flow only if $Re_\tau > 40\,000$ and only in the range $100\delta_\nu < y < \delta/100$. Using the attached eddy model's $E^+ \approx M_0 + M_1 \ln(\delta/y)$ in the range $y_* < y \ll \delta$ we obtain the following asymptotic form of the mean flow profile in $y_* < y < 0.01\delta$ (as y_* is larger than $100\delta_\nu$):

$$\overline{u}_+ \approx C_s M_0 \ln(y/\delta) - \frac{C_s M_1}{2}[\ln(y/\delta)]^2 + M_2 \tag{6.4}$$

in terms of an extra integration constant M_2. We stress again the limited y-range of validity of this high-Reynolds-number mean flow profile (to the right of the outer peak) and that it can only be expected at $Re_\tau > 40\,000$. This y-range can be made longer if we do not use $-\langle u'v'\rangle \approx u_\tau^2$ which leads to (6.3) but $-\langle u'v'\rangle \approx u_\tau^2 \approx 1 - y/\delta$ which holds for y/δ_ν larger than $O(100)$ and leads to $(1 - y/\delta)(\mathrm{d}\overline{u}_+/\mathrm{d}\ln y^+) \approx C_s E^+$ in place of (6.3).

As shown in § 5, $E^+ \approx M_0 + M_1 \ln(\delta/y)$ and therefore also (6.4) are based on the additional assumption that any intermittency which might exist in the fluctuating wall shear stress is of such a nature that the Townsend–Perry spectral scalings $E_{11}(k_1, y) \sim u_\tau^2 k_1^{-1}$ remain intact. Otherwise one can expect power laws of y/δ instead of logarithms of y/δ in the formula for the mean flow profile (6.4).

We close this section with a comment on the mesolayer, a concept introduced by Long & Chen (1981) and most recently discussed by Vallikivi, Ganapathisubramani & Smits (2014) who also provide a list of relevant references. In the present paper, profiles have been obtained for $\overline{u'^2}(y)$ in the range $\delta_\nu \ll y \ll \delta$ and for $\overline{u}(y)$ in the range $y_{P\epsilon} < y < 0.01\delta$ where production has been assumed to balance dissipation. George & Castillo (1997) argued that the mesolayer is a region from $y^+ \simeq 30$ to $y^+ \simeq 300$ where, owing to low turbulent Reynolds number y^+ values, the dissipation does not have its high-Reynolds-number scaling and the Kolmogorov range (iv) of our spectral model in § 4 is effectively absent. This has no bearing on our calculations of §§ 4 and 5 because the energy in the Kolmogorov range (iv) is small compared with the other ranges and the outer peak comes from the new small wavenumber range (ii). (In fact it is easy to check that the Kolmogorov range in the Townsend–Perry model cannot, by itself, lead to an outer turbulent energy peak.) However, it might be that we cannot use the scaling $\tau \sim y/u_\tau$ at $y^+ \lesssim 300$ and that our approach for obtaining the mean flow gradient profile might therefore be valid only in the region $\max(300\delta_\nu, y_{P\epsilon}) < y \ll 0.01\delta$. Note that the value of y_{peak} in the Princeton NSTAP data is about $300\delta_\nu$

at $Re_\tau \approx 40\,000$ and about $500\delta_\nu$ at $Re_\tau \approx 100\,000$, which means that the mesolayer is indeed under y_{peak} for $Re_\tau > 40\,000$. The prediction that the mean flow gradient has an outer peak at the same distance from the wall where the streamwise turbulence intensity has an outer peak has been based on the assumption that $y_{P\epsilon} < y_{peak}$. The region where production and dissipation balance and where turbulent transport has negligible effects may or may not be expected to have an overlap with the mesolayer. The task of working out the scalings of $y_{P\epsilon}$ and how it compares with $300\delta_\nu$ must be left for a future study which will have the means to address these questions.

7. Conclusion

In way of conclusion we list the main points made in this paper.

(i) For the Townsend–Perry k_1^{-1} spectrum to be viable, i.e. to be compatible with a realistic integral scale dependence on y, we need to add to the Perry *et al.* (1986) spectral model an extra wavenumber range at wavenumbers smaller than those where $E_{11}(k_1, y) \sim u_\tau^2 k_1^{-1}$.

(ii) Simple modelling of this range (see § 4) implies the existence of an outer peak in the streamwise turbulence kinetic energy at a y-position y_{peak} which grows with respect to δ_ν and decreases with respect to δ as Re_τ increases. The streamwise kinetic energy at that peak grows logarithmically with Re_τ.

(iii) The functional form which results from our modified Townsend–Perry model and which may be useful as a starting point in future investigations is the following: in the range $\delta_\nu \ll y < y_* \sim \delta Re_\tau^{-1/3}$

$$\tfrac{1}{2}\overline{u'^2}(y)/u_\tau^2 \approx C_{s0} - C_{s1}\ln(\delta/y) - C_{s2}(y/\delta)^d Re_\tau^{d/3} \tag{7.1}$$

where all of the constants are independent of y, δ, ν and Re_τ except for C_{s0} which may be a logarithmically increasing function of Re_τ; in the range $y_* < y \ll \delta$

$$\tfrac{1}{2}\overline{u'^2}(y)/u_\tau^2 \approx C_3 + C_4\ln(\delta/y) \tag{7.2}$$

as predicted by Townsend (1976) and Perry *et al.* (1986).

(iv) The very high-Re_τ Princeton Superpipe NSTAP data used here and the turbulent channel flow DNS of Dallas *et al.* (2009) support the view that it is the eddy turnover time $\tau \equiv E/\epsilon$ that is independent of ν and δ in the range $\delta_\nu \ll y \ll \delta$ rather than the mean flow gradient. This implies $\tau \sim y/u_\tau$ in that range, a relation which can serve as a unifying principle across Reynolds numbers in turbulent pipe/channel flows. Of course, further research is needed to fully establish such a unifying principle.

(v) The mean flow profile and scalings can be obtained from $\tau \sim y/u_\tau$ if enough is known about the production–dissipation balance/imbalance. Here we have assumed that production and dissipation balance in a range $y_{P\epsilon} < y \ll \delta$ where $y_{P\epsilon}$ is smaller than y_{peak}. Due to this balance, a profile for E^+ similar to that of $\overline{u'^2}/u_\tau^2$ implies that $(1 - y/\delta - (\mathrm{d}\overline{u}_+/\mathrm{d}y^+))(\mathrm{d}\overline{u}_+/\mathrm{d}\ln y^+)$ (i) has an outer peak at the same position $y = y_{peak}$ where $\overline{u'^2}/u_\tau^2$ has an outer peak, and (ii) decreases with distance from the wall as a function of $\ln(\delta/y)$ where $y_* < y \ll \delta$. In the intermediate range of wall distances where $-\langle u'v'\rangle \approx u_\tau^2$ is a good approximation (see point 6 below), these two conclusions hold for $\mathrm{d}\overline{u}_+/\mathrm{d}\ln y^+$. The very high Re_τ NSTAP Princeton Superpipe data show clear evidence in support of these conclusions.

(vi) The same data also show that the Reynolds stress $\langle u'v' \rangle$ is approximately equal to $-u_\tau^2$ only if $Re_\tau > 40\,000$ and for distances from the wall such that $100 < y^+$, $y/\delta < 0.01$. The balance $-\langle u'v' \rangle (\mathrm{d}\overline{u}/\mathrm{d}y) \approx \epsilon$ and the kinetic energy profile $E^+ \approx M_0 + M_1 \ln(\delta/y)$ (where M_0 and M_1 are dimensionless constants) in $y_* \ll y \ll \delta$ therefore imply in terms of an integration constant M_2 that

$$\overline{u}_+ \approx C_s M_0 \ln(y/\delta) - \frac{C_s M_1}{2} [\ln(y/\delta)]^2 + M_2 \tag{7.3}$$

in $y_* < y < 0.01\delta$ provided that $Re_\tau > 40\,000$. This is the modified log-law of the wall.

Acknowledgements

We are very grateful to Dr M. Vallikivi and Professor A. J. Smits for kindly providing us with their NSTAP Superpipe data (first published in Hultmark *et al.* 2012, 2013) and with energy spectra from the same measurements. This work was supported by Campus International pour la Sécurité et l'Intermodalité des Transports, la Région Nord-Pas-de-Calais, l'Union Européenne, la Direction de la Recherche, Enseignement Supérieur, Santé et Technologies de l'Information et de la Communication et le Centre National de la Recherche Scientifique. J.C.V. acknowledges the support of an ERC advanced grant (2013–2018).

REFERENCES

ALFREDSSON, P. H., JOHANSSON, A. V., HARITONIDIS, J. & ECKELMANN, H. 1988 The fluctuating wall shear-stress and the velocity field in the viscous sublayer. *Phys. Fluids* **31**, 1026–1033.

DEL ALAMO, J. C. & JIMENEZ, J. 2009 Estimation of turbulent convection velocities and corrections to Taylor's approximation. *J. Fluid Mech.* **640**, 5–26.

BAILEY, S. C. C. & SMITS, A. J. 2010 Experimental investigation of the structure of large- and very-large-scale motions in turbulent pipe flow. *J. Fluid Mech.* **651**, 339–356.

DALLAS, V., VASSILICOS, J. C. & HEWITT, G. F. 2009 Stagnation point von Kármán coefficient. *Phys. Rev.* E **80**, 046306.

FERNHOLZ, H. H. & FINLEY, P. J. 1996 The incompressible zero-pressure gradient boundary layer: an assessment of the data. *Prog. Aerosp. Sci.* **32**, 245–311.

FRISCH, U. 1995 *Turbulence*. Cambridge University Press.

GEORGE, W. K. & CASTILLO, L. 1997 Zero-pressure gradient turbulent boundary layer. *Appl. Mech. Rev.* **60**, 689–729.

HULTMARK, M., VALLIKIVI, M., BAILEY, S. C. C. & SMITS, A. J. 2012 Turbulent pipe flow at extreme Reynolds numbers. *Phys. Rev. Lett.* **108**, 094501.

HULTMARK, M., VALLIKIVI, M., BAILEY, S. C. C. & SMITS, A. J. 2013 Logarithmic scaling of turbulence in smooth- and rough-wall pipe flow. *J. Fluid Mech.* **728**, 376–395.

HUTCHINS, N. & MARUSIC, I. 2007 Evidence of very long meandering features in the logarithmic region of turbulent boundary layers. *J. Fluid Mech.* **579**, 1–28.

KOLMOGOROV, A. N. 1962 A refinement of previous hypotheses concerning the local structure of turbulence in a viscous incompressible fluid at high Reynolds number. *J. Fluid Mech.* **13**, 82–85.

LONG, R. R. & CHEN, T. C. 1981 Experimental evidence for the existence of the mesolayer in turbulent systems. *J. Fluid Mech.* **105**, 9–59.

MORRISON, J. F., MCKEON, B. J., JIANG, W. & SMITS, A. J. 2004 The scaling of the streamwise velocity component in turbulent pipe flow. *J. Fluid Mech.* **500**, 99–131.

ÖRLÜ, R. & SCHLATTER, P. 2011 On the fluctuating wall-shear stress in zero pressure-gradient turbulent boundary layer flows. *Phys. Fluids* **23**, 021704.

PERRY, A. E., HENBEST, S. M. & CHONG, M. S. 1986 A theoretical and experimental study of wall turbulence. *J. Fluid Mech.* **165**, 163–199.

POPE, S. B. 2000 *Turbulent Flows*. Cambridge University Press.

ROSENBERG, B. J., HULTMARK, M., VALLIKIVI, M., BAILEY, S. C. C. & SMITS, A. J. 2013 Turbulence spectra in smooth- and rough-wall pipe flow at extreme Reynolds numbers. *J. Fluid Mech.* **731**, 46–63.

SMITS, A. J., MCKEON, B. J. & MARUSIC, I. 2011 High Reynolds number wall turbulence. *Annu. Rev. Fluid Mech.* **43**, 353–375.

TENNEKES, H. & LUMLEY, J. L. 1972 *A First Course in Turbulence*. MIT Press.

TOMKINS, C. D. & ADRIAN, R. J. 2003 Spanwise structure and scale growth in turbulent boundary layers. *J. Fluid Mech.* **490**, 37–74.

TOWNSEND, A. A. 1976 *The Structure of Turbulent Shear Flows*. Cambridge University Press.

VALLIKIVI, M., GANAPATHISUBRAMANI, B. & SMITS, A. J. 2014 Spectral scaling in boundary layers and pipes at very high Reynolds numbers. *J. Fluid Mech.* **771**, 303–326.

ZHAO, R. & SMITS, A. J. 2007 Scaling of the wall-normal turbulence component in high-Reynolds-number pipe flow. *J. Fluid Mech.* **576**, 457–473.